Evaluation of ATR−FTIR Spectroscopy as an "in Situ" Tool for Following the Hydrolysis and Condensation of Alkoxysilanes under Rich H_2O Conditions

M. Isabel Tejedor-Tejedor,* Liana Paredes, and Marc A. Anderson

Water Chemistry Program, University of Wisconsin, 660 North Park Street, Madison, Wisconsin

Received March 9, 1998. Revised Manuscript Received July 28, 1998

The fate of ~0.5 M tetraethyl orthosilicate (TEOS) in HNO_3 solutions (pH 2−3) was followed by "in situ" ATR−FTIR spectroscopy. ATR spectra with excellent signal-to-noise ratios were obtained with collection times of 2 min. A qualitative examination of spectra measured at different reaction times showed that TEOS was first converted into ethanol and $Si(OH)_4$, and then amorphous SiO_2 was precipitated from the solution. The TEOS hydrolysis rate increased with decreasing pH of the nitric solution. In addition, under reaction conditions that make the system homogeneous (stable micelles, solution, or stable suspension), the use of standards enabled measurement of concentrations of the reactant products: EtOH, $Si(OH)_4$, and SiO_2. Calibration curves for EtOH in water and in methanol, for TEOS in ethanol, and for SiO_2 in water fit equations of the form $y = bx$, with R^2 values between 0.999 and 0.99. The mass balance on the acidified TEOS/water systems was good: initial concentrations of 0.56 F of TEOS resulted in [EtOH] = 2.12 M and [SiO_2] = 0.53 M.

1. Introduction

The microstructure of Si−X gels prepared by hydrolysis and condensation of alkoxysilanes has been linked to both the synthesis parameters (e.g.: pH, water/alkoxysilane ratio, nature of the alkoxide, etc.) as well as to the aging, drying and sintering conditions. In general, acid-catalyzed systems involving low water/alkoxysilane ratios generate branched polymeric sols, while spherical colloids are formed in base-catalyzed systems with higher water/alkoxysilane ratios. Numerous speciation studies on silica sol−gel systems[1−4] have shown that synthesis parameters, such as the water/alkoxysilane ratio, pH of catalysis, solvent nature of the alkoxide precursor etc., influence the path of hydrolysis and condensation.

In early studies, the kinetics of hydrolysis and condensation of silicon alkoxides have been followed by using analytical techniques that required wet chemistry manipulation such as distillation/titration of the generated alcohol, colorimetric titration of silica products, or paper chromatography.[2] In the last 10 years, however, ^{29}Si NMR has been the most singly used technique to identify the different Si containing species produced in sol−gel processes.[1−8] This spectroscopic technique is a very powerful tool which can differentiate among silicon atoms attached to different combinations of ligands. In addition, ^{29}Si NMR can quantitatively monitor Si sites with different connectivity and, therefore, determine concentration distribution of small oligomers present in the system, as well as whether these oligomers are cyclic, linear, or branched.

However, the high specificity of this technique is not equaled by its sensitivity. The low natural abundance of ^{29}Si, low gyromagnetic ratio, and the rather long relaxation times make ^{29}Si NMR spectroscopy a less sensitive "in situ" tool for following these hydrolysis and condensation reactions in real time. The low sensitivity can be circumvented by isotopic enrichment, by adding paramagnetic transition metal complexes as $Cr(acac)_3$ to the system to reduce the relaxation time, and/or by accumulating many pulses.[1,6,7] Since the first proposition is too expensive to be used routinely, a combination of the latter techniques is commonly used in order to obtain good signal-to-noise ratios. The data collection time for a reasonable signal-to-noise ratio in ^{29}Si NMR spectroscopy depends on concentration of the silicon species and the mobility of these species, since condensed phases produce weaker signals. The majority of the reported studies on the kinetics of hydrolysis and condensation by ^{29}Si NMR are related to systems with alkoxide concentrations near 2 M. To obtain acceptable signal-to-noise ratios, the authors use a combination of best pulse time and number of accumulated FID's (free induction decay), which generally result in a collection

* To whom correspondence should be addressed. Telephone: (608) 262-0365. E-mail: tejedor@engr.wisc.edu.

(1) Li Voon Ng, L.; Thompson, P.; Sanche, J.; Macosko, Ch. W.; McCormick, A. V. *Macromolecules* **1995**, *28*, 6471.
(2) Brinker, C. J.; Scherer, G. W. *Sol−Gel Science. The Physics and Chemistry of Sol−Gel Processing;* Academic Press: Boston, MA, 1990.
(3) Bernards, T. N. M.; van Bommel, M. J.; Boonstra, A. H. *J. Non-Cryst. Solids* **1991**, *134*, 1.
(4) van Beek, J. J.; Seykens, D.; Jansen, J. B. H.; Schuiling, R. D. *J. Non-Cryst. Solids* **1991**, *134*, 14−22.
(5) Brunet, F.; Cabane, B. *J. Non-Cryst. Solids* **1993**, *163*, 211.
(6) Marsmann, H. ^{29}Si NMR Spectroscopic Results. In *NMR Basic Principles and Progress*; Diehl, P., Fluck, E., Kosfeld, R., Eds.; Springer-Verlag: New York, 1981.
(7) Boonstra, A. H.; Bernards, T. N. M. *J. Non-Cryst. Solids* **1989**, *108*, 249.
(8) Šefčík, J.; McCormick, A. V. *Catal. Today* **1997,** *35*, 205.

10.1021/cm980146l CCC: $15.00
Published on Web 10/07/1998

time of approximately 14 min. The better quality data belong to systems having high concentrations of total silicon, substoichiometric water/alkoxide ratios and very low pH conditions for hydrolysis. These experimental conditions allow for only limited and slow hydrolysis and condensation. Despite these limitations, Šefčík and McCormick[8] have used the existing pool of ^{29}Si NMR data in the literature to model the kinetics and thermodynamics for TEOS polymerization in water/ethanol solutions. However, Boonstra and Bernards[7] believe that the time required to collect a spectrum with good signal-to-noise ratio, even for these type of systems, is longer than that desired for following the initial rate of hydrolysis. To obtain data that represent the system at very short time of reaction, these authors quench the reaction, by cooling very quickly to below −100 °C. They then measure the ^{29}Si NMR spectrum at −75 °C.

Our research group is interested in following the reaction path of systems that have a total silicon concentration of approximately 0.5 M, a very high water/alkoxide molar ratio (80:1), and pH values in the vicinity of 3 and 11. As mentioned above, these systems would not be good candidates for ^{29}Si NMR with any acceptable degree of resolution for the study of reaction kinetics. Therefore, in this paper, we will explore the analytical capabilities of aqueous vibrational spectroscopy for the "in situ" study of these systems.

IR and Raman spectroscopy could be regarded as well as powerful tools for the "in situ" identification of chemical species present in these water/alkoxysilanes mixtures. Both techniques provide complementary information concerning vibrational spectra of chemical groups. Although Raman is a much weaker phenomenon than IR and its use is limited to systems optically transparent in the visible, it has, however, been used by several authors to investigate the hydrolysis and condensation of TMOS and TEOS,[9] and also to determine the structure of silicate species in very alkaline aqueous solutions.[10,11] IR spectroscopy, on another hand, has been widely used in the study of solid silicates and silica gels,[2,12] but very little effort has been devoted to identifying silicon species in aqueous solutions or suspensions. The historical reason for the paucity of IR data in aqueous/alcoholic mediums is associated with the strong absorption of radiation by water in several regions of the mid and far IR. Only aqueous solutions or suspensions with very short path lengths would be optically transparent and would allow one to see the vibrational spectra of chemical species in these systems. Fortunately, since the mid-80's, aqueous IR spectroscopy has become a routine technique for the analysis of chemical groups in solution. The increased use of IR was due to the combination of FTIR spectroscopy with sensitive attenuated total reflection (ATR) sampling devices such as the cylindrical internal reflectance (CIR) cell.[13,14] Moreover, CIR−FTIR spectroscopy has proven to be a very useful technique in the study of aqueous colloids,[15] and even quantitative analysis can be performed with CIR−FTIR in the case of stable colloidal suspensions.[16]

The hydrolysis process can be followed by examining the transformation of alkoxides into alcohol. In theory, silicon species with different degrees of hydrolysis will have different symmetries and thus should produce different IR spectra. This paper is addressed to demonstrating the value of this technique in the study of the hydrolysis and condensation reactions in a sol−gel process.

2. Experimental Section

2.1. Preparation of the Systems Studied by CIR−IR. *Reagents and Materials.* Tetraethyl orthosilicate (TEOS): Aldrich Chemical Inc. 98%; Nitric acid: Fisher, ACS reagent, 70%; Methanol: Fisher, Chemical HPLC grade, 99.9%; Ethanol: Pharmco, dehydrated 200 proof; Tetramethyl orthosilicate (TMOS): Aldrich Chemical Inc. 98%; Water: Nanopure 18 MΩ; Dialysis Membrane tubing: Spectra/por, molecular cutoff = 3500 mw. (dialysis tubing was employed to clean the sol after the hydrolysis and condensation reactions were complete).

Standards Used in the Preparation of Calibration Curves. Samples of known concentration were used to establish the relationship between absorption and concentration for ethanol in water, ethanol in methanol, TEOS in ethanol, water in methanol, and suspensions of SiO_2 in aqueous solution. The standard solutions were prepared using chemicals described in the above paragraph, none of which are primary standards. SiO_2 suspensions were prepared by the hydrolysis of TEOS in aqueous media followed by dialysis in 18 MΩ Nanopure UV water at the desired pH. The final concentration of SiO_2 in the suspensions was measured gravimetrically.

Hydrolysis of TEOS in Aqueous Medium. A 4.5 mL sample of TEOS was added to 30 mL of nitric acid solutions of pH values of either 3, 2.5, or 2, resulting in a formal silicon concentration of 0.58 M. The two liquid phase mixtures were vigorously stirred for several hours. In seconds, the TEOS developed into a micellar suspension in the aqueous phase. The time for the milky emulsion to transform into a clear solution/sol ranged between 27 min for the system at pH 2 to 90 min for the system at pH 3. Aliquots of these mixtures at different times of preparation were withdrawn from the reaction vessel and deposited in the CIR boat for obtaining IR spectra.

After 24 h of reaction, a fraction of the system hydrolyzed at pH 3 was transferred into membrane tubing and dialyzed against a nitric acid solution of pH 2 to remove the ethanol byproduct. This SiO_2 suspension was then used to prepare the CIR−FTIR calibration curve.

Hydrolysis of TEOS in Methanol. A 4.5 mL sample of TEOS was added to 29.75 mL of methanol, and after this solution was chilled, 1 mL of a 0.37 N HNO_3 solution was added at once. The mixing of HNO_3 with the solution is exothermic, and the temperature of the mixture increased suddenly to nearly 20 °C. This reacting mixture looks like a transparent, nonviscous liquid from the moment of mixing until several days later.

2.2. Infrared Spectroscopy. The CIR infrared spectra of the systems mentioned above were recorded interferometrically with a Nicolet Magna 750 Series II spectrometer and using an MCT-A detector. The ATR accessory used was a Spectra Tech CIRCLE, outfitted with a metal boat. A ZnSe crystal rod, which produces an effective angle of incidence of 46°, was used as the internal reflectance element (IRE). Single beam spectra were the result of averaging either 200 (in the hydrolysis of TEOS) or 500 co-added interferograms (this is

(9) Gnado, J.; Dhamelincourt, P.; Pelegris, C.; Traisnel, M.; le Maguer Mayot, A. *J. Non-Cryst. Solids* **1996**, *208*, 247.
(10) Dutta, P. K.; Shieh, D. *Appl. Spectrosc.* **1985,** *39*, 343.
(11) Freund, E. *Bull. Soc. Chim. Fr.* **1973**, *7−8*, 2244.
(12) Tripp, C. P.; Hair, M. L. *Langmuir* **1995**, *11*, 1, 149.
(13) Wong, J. S.; Rein, A. J.; Wilks, D.; Wilks, P. *Appl. Spectrosc.* **1984,** *38*, 32.
(14) Süer, M. G.; Dardas, Z.; Ma, Y. H.; Moser, W. R. *J. Catal.* **1996**, *162*, 320.
(15) Tejedor-Tejedor, M. I.; Anderson, M. A. *Langmuir* **1990,** *6*, 602.
(16) Tickanen, L. D.; Tejedor-Tejedor, M. I.; Anderson, M. A. *Langmuir* **1991,** *7*, 451.

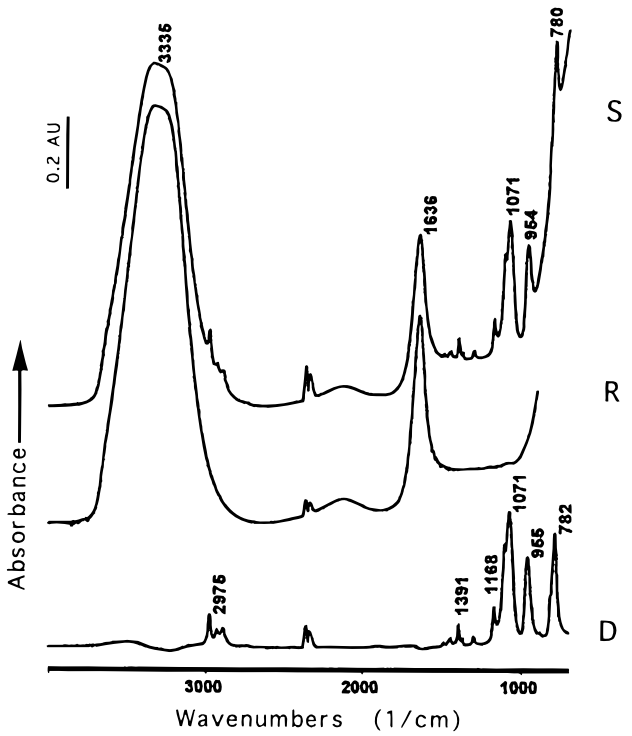

Figure 1. CIR−FTIR spectra: (S) TEOS in H_2O; (R) H_2O; (D) difference spectrum (S minus R).

equivalent to 2−5 min of collection time). The spectral resolution was 4 cm^{-1}.

Methodology. Single-beam IR spectra were collected successively for the empty boat (background), the solvent (reference), and either the solutions/suspensions of known concentrations or the reacting TEOS systems (sample). The background, reference, and sample spectra of a system were recorded without moving the sample holder to prevent any change in the angle of incidence (θ) and the number of internal reflections (N). The same background and reference spectra were used for the data reduction of all standard spectra of a calibration curve.

The reacting TEOS systems were stirred on a magnetic plate from the moment of mixing until they were used in IR measurements. In the early stages of the reaction, the acidified TEOS/water systems consisted of two immiscible phases. Two-phase samples were stirred by pipet plunging during the IR data collection, to maintain a fine emulsion of TEOS in H_2O. Background and reference were common for all the spectra of the same TEOS reaction collected at different reaction times, but for a time span no longer than 3 or 4 h. The time of reaction (t_r) was considered to be the interval from the moment of mixing (t_o) to half of the time for IR spectrum collection.

Data Reduction. Single-beam spectra of the samples and references were divided against the spectrum of the empty boat to obtain the pATR spectra. The reference spectra multiplied by the adequate factor ([absorbance of solvent in reference] × [factor] = [absorbance of solvent in sample]) were subtracted from the corresponding sample spectra. Using this type of data reduction, the absorption bands for the species of interest, namely reactants and products in the hydrolysis of TEOS are more evident in the pATR spectra, as is shown in Figure 1. The same methodology is used to isolate the spectral features of standards used in the preparation of the calibration curves.

3. Results and Discussion

3.1. Description of Acidified TEOS/H_2O (Molar Ratio = 1:80) Systems. Figure 2 shows the ternary phase diagram of the TEOS−EtOH−H_2O system.[2] Point A illustrates the starting point of our sol−gel reaction

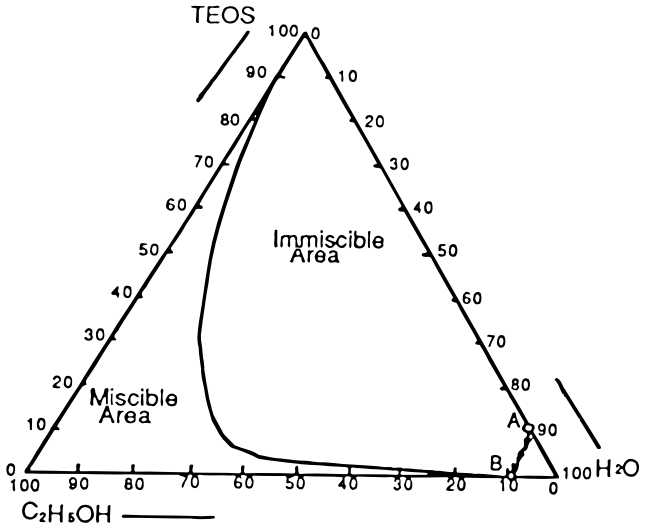

Figure 2. TEOS, H_2O, and 95% EtOH ternary phase diagram at 25 °C. A represents the starting composition of a TEOS:H_2O (1:86) system. B illustrates the final composition of this system after equilibration.

system with a TEOS:H_2O molar ratio of 1:80. Over the course of the reaction, the composition progresses to point B by the consumption of TEOS and the formation of an EtOH byproduct. At the start of the reaction, the hydrolysis occurs only at the alkyl silicate droplet−water interface as follows:

$$-\mathrm{Si(OEt)_4} + n\mathrm{H_2O} \xrightarrow{\mathrm{H^+}} \mathrm{Si(OH)}_n\mathrm{(OEt)}_{4-n} + n\mathrm{EtOH} \quad (1)$$

Once produced, the $Si(OH)_n(OEt)_{4-n}$ species enter the water phase. As the concentration of hydrolyzed products increases, condensation reactions are expected to take place as described by eq 2. Following the phase

$$-\mathrm{Si-OH-} + \mathrm{OH-Si-} \xrightarrow{\mathrm{H^+}} -\mathrm{Si-O-Si-} + \mathrm{H_2O} \quad (2)$$

diagram of Figure 2, the majority of the reaction process should take place under a two-phase condition. In this case, the hydrolysis rate can be significantly influenced by the size of the emulsion droplets (concentration of sites) and thus, by the degree and nature of stirring.

For the reaction conditions of TEOS:H_2O molar ratio 1:80, we expect the alkyl silicates to be thoroughly hydrolyzed, and the solubility product for silica should be exceeded at some point during this reaction. Under these conditions, a nucleation process can be used to describe the formation of particles, as discussed many years ago by Iler.[17]

3.2. Identification of Chemical Species in the ATR−FTIR Spectra of the Acidified TEOS/H_2O Systems. *Organic Species.* The CIR−FTIR spectra of TEOS and EtOH are shown in Figure 3. Observed frequencies and assignments, from several literature sources, are listed in Table 1. C−H stretching vibrations of TEOS and EtOH are located between 3000 and 2800 cm^{-1} and they have a moderate to weak intensity; the OH stretching of the EtOH appears as a broad band at 3320 cm^{-1}, and the width and the exact location of

(17) Iler, R. K. *The Chemistry of Silica*; John Wiley & Sons: New York, 1979.

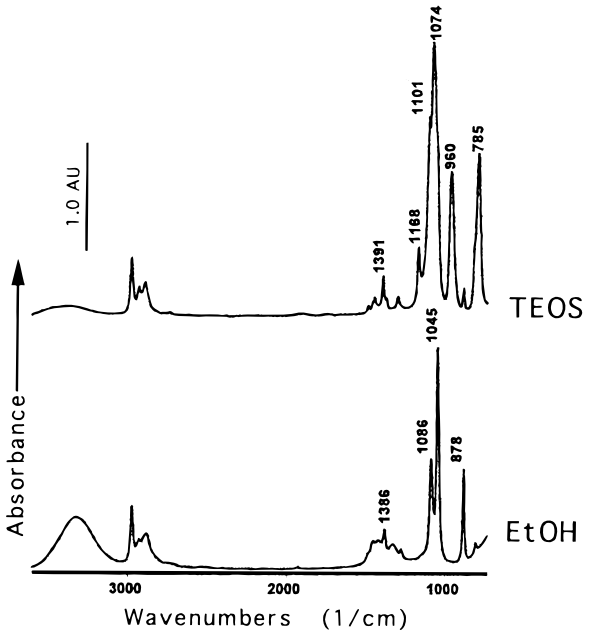

Figure 3. CIR−FTIR spectra of EtOH (neat) and TEOS (TEOS in EtOH 80% V).

Table 1. Observed Frequencies and Band Assignment for Tetraalkoxysilanes and the Corresponding Alcohols

	frequency at max. (cm^{-1})			
vibrational mode	CH_3OH	C_2H_5OH	$(C_2H_5O)_4Si$	$(CH_3O)_4Si$
ν(O−H)	3320			
ν(C−H)	2943	2981	2975	2951
ν(C−H)		2935	2929	
ν(C−H)	2832	2904	2890	2848
$\delta_a(CH_3) + \delta_a(CH_2)$	1494	1455	1484	1466
$\delta'_a(CH_2)$			1443	
δ(OH) + $\delta_a(CH_3)$	1415[c]	1419[a]		
$\delta_s(CH_3)$		1386[b]	1391	
$\omega(CH_2)$		1327[a]	1366	
$\tau(CH_2)$		1275[b]	1296	
$\rho(CH_3)$	1113		1168[e]	1196
$\rho'(CH_3)$		1086[b]	1101[e,f]	
ν(C−O)/(C−O) + (C−C)	1023	1045[b]	1073[d−f]	1094[g]
ν(C−C)/(C−O)		878		
$\rho(CH_3)$			960[d,e]	
ν(Si−O)			785[d−f]	838[g,h]

[a] EtOH. Mikawa:[18] 1419 cm^{-1} to $\omega(CH_2)$; 1327 cm^{-1} to δ(OH). [b] EtOH. Allinguer:[19] 1386 to $\omega(CH_2) + \delta(CH_3)$; 1086 cm^{-1} to ν(C−O)/(C−C); 1045 cm^{-1} to $\rho(CH_3) + \rho(CH_2)$; 1290 cm^{-1} to δ(OH). [c] MeOH. Allinguer:[19] 1415 cm^{-1} to $\delta(CH_3)$; the δ(OH) is attributed to a band at 1340 not visible in our spectrum. [d] TEOS. Mondragon:[20] 1073 cm^{-1} to ν_a(Si−O)/ν_a(C−O); 785 cm^{-1} to ν_a(C−O)/ν_a(Si−O); 960 cm^{-1} to ν(C−C). [e] TEOS. van der Vis:[21] 1101 and 1073 cm^{-1} to ν_a(C−O)(E and B); 785 cm^{-1} to ν(Si−O); 960 cm^{-1} to $\rho(CH_3)$. [f] TEOS. Ypenburg:[22] 1101 and 1073 cm^{-1} to ν_a(C−O). [g] TMOS: Ypenburg:[22] 1094 cm^{-1} to ν_a(C−O); 838 cm^{-1} to ν_a(Si−O). [h] TMOS. Ignatyev:[23] 1094 and 838 cm^{-1} to ν(C−O)/ν(Si−O).

this band should be very sensitive to the degree of association and therefore to the matrix. Methyl and methylene deformations as well as methylene wagging and twisting and the OH in-plane deformation appear between 1450 and 1274 cm^{-1} and show a weak to moderate intensity.[18−24] C−C and C−O stretching, in addition to methyl and methylene rocking, appear in the region 1200−800 cm^{-1}. The spectra of Figure 3 show that this region exhibits the most intense bands of TEOS and EtOH spectra, in addition to major differences between the two spectra. Therefore, this spectral region provides the largest sensitivity and specificity for the analysis of these species.

Table 1 shows that there is not a general consensus among the authors in relation to the assignments of some of the observed frequencies of the TEOS spectrum in this region. This circumstance could be a barrier to the interpretation of structural changes of these species during the reaction. However, this is not an issue for the purpose of identification and quantitative determination of TEOS and EtOH in the reaction mixture. Bands at 1168, 960, and 785 cm^{-1} are present only in the spectrum of TEOS and do not overlap with absorption bands of the spectrum of EtOH. Moreover, the band at 878 cm^{-1} of the EtOH spectrum, ν_s(C−C + C−O), is not present in the spectrum of TEOS, and neither does it have the potential for overlapping with other TEOS bands (see Figure 3). Therefore, it should be easy to identify these species in the presence of each other.

Silicon Oxide Species. The purpose of this section is to establish the differences in the IR spectra of monomeric silicic acid, polymeric chains, and tridimensional SiO_2 in aqueous media. Figure 4 shows the CIR−IR spectra of monomeric and polymeric silicon oxide species in aqueous solution/suspensions, in the region 1400−700 cm^{-1}. According to the literature,[24−27] the stretching modes of Si−O for different species of silicon oxide/hydroxide should appear between 1200 and 800 cm^{-1}.

The spectrum of dissolved SiO_2 in H_2O (1.7 mM; pH = 5.5), Figure 4a, shows a unique peak at 942 cm^{-1}. Under these solution conditions, $Si(OH)_4$ is the major silicon oxide species. Since this molecule has a T_d symmetry, only the ν_d(SiO) mode related to the SiO_4 tetrahedron should absorb in this spectral region. The frequency observed in the spectrum of Figure 4a appears at slightly lower frequencies than the corresponding mode of the SiO_4^{4-} ion, reported at 956 cm^{-1} in the literature.[25] Silicic acid, in addition to the vibrations of the SiO_4 tetrahedron, has vibrational modes related to the −SiOH groups, and the in-plane deformation mode (δ(OH)) of this group is also active in this region. This vibration appears at 1065 ± 35 cm^{-1} as a weak broad band.[24] Although the spectrum Figure 4a shows such a band, its assignment is uncertain since the absorption intensity in this region is very close to the detection limit of the technique.

The spectrum of Figure 4b corresponds to a solution 0.08 M of Na_2SiO_3 in 2 M NaCl, at pH 12. Under these

(18) Mikawa, Y.; Brasch, J. W.; Jakobsen, R. J. *Spectrochim. Acta* **1971**, *27A*, 529.
(19) Allinguer, N. L.; Rahman, M.; Lii, J.-H. *J. Am. Chem. Soc.* **1990**, *112*, 8293.
(20) Mondragon, M. A.; Castaño; Garcia M., J.; Tellez S., C. A. *Vibr. Spectrosc.* **1995**, *9*, 293.
(21) van der Vis, M. G. M.; Konings, R. J. M.; Oskam, A.; Snoeck, T. L. *J. Mol. Struct* **1992**, *274*, 47.
(22) Ypenburg, J. W.; Gerding, H. *Recl. Trav. Chim. Pays-Bas* **1972**, *91*, 1245.
(23) Ignatyev, I. S.; Lazarev, A. N.; Tenisheva, T. F.; Shchegolev, B. F. *J. Mol. Struct.* **1991**, *244*, 193.
(24) Roeges, N. P. G. *A Guide to the Complete Interpretation of Infrared Spectra of Organic Structures*; John Wiley & Sons: New York, 1994.
(25) Nakamoto, K. *Infrared and Raman Spectra of Inorganic and Coordination Compounds*, 5th ed.; John Wiley & Sons: New York, 1997; Part B.
(26) Etchepare, J. *Spectrochim. Acta* **1970**, *26A*, 2174.
(27) Efimov, A. M. *Optical Constants of Inorganic Glasses*; CRC Press: New York, 1995.

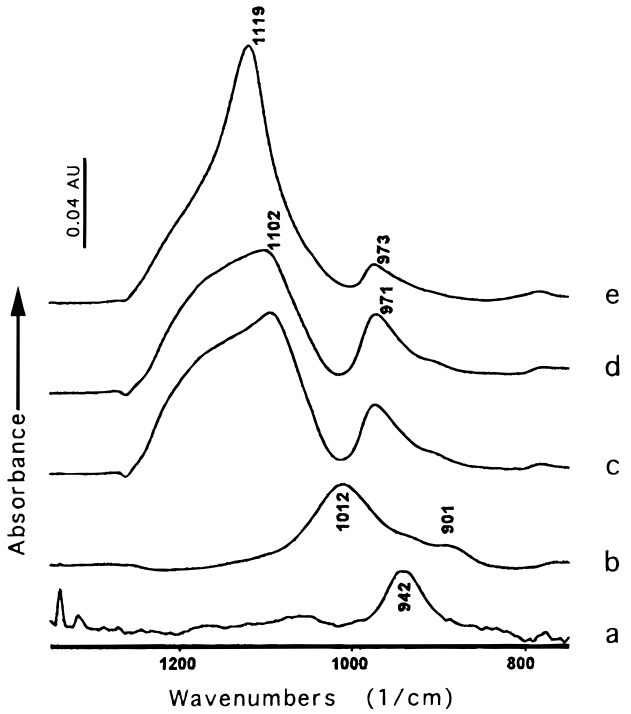

Figure 4. CIR−FTIR difference spectra of silicon oxide species in aqueous media (spectrum solution or suspension minus spectrum of water): (a) 1.7×10^{-3} M $Si(OH)_4$, pH = 5.5 (40×); (b) 0.08 M Na_2SiO_3 at pH 12; (c and d), SiO_2 sol from acid hydrolysis of TEOS, dialyzed in HNO_3 solution of pH 2 (c) and pH 3 (d), respectively; (e) SiO_2 sol from basic hydrolysis of TEOS, dialyzed in H_2O.

conditions, 80% of the silicate should be as $Si_4O_8(OH)_4^{4-}$ and 20% as $SiO(OH)_3$.[28] The ν_a(Si−OSi) mode of a cyclic chain silicate, such as the $Si_4O_8(OH)_4^{4-}$ ion, should appear between 1000 and 1050 cm^{-1} with a large relative intensity, while the ν_s(Si−OSi) mode should be associated with a weaker absorption band near 700 cm^{-1}, and the ν(Si−O−) mode should absorb between 880 and 940 cm^{-1}.[9,25,26] In the spectrum of $Si_4O_8(OH)_4^{4-}$ ions in aqueous solution these modes absorb at 1012, 740, and 901 cm^{-1}; see Figure 4b.

Spectra of Figure 4c−e belong to SiO_2 particles in aqueous suspensions. The absorption band in the region of 1100 cm^{-1} and the shoulder at 1200 cm^{-1} are acknowledged to originate from two different vibrations of the SiOSi bridge[27] of silica glass (α-quartz: 1070 and 1160 cm^{-1}), although some authors believe that these two bands are due to the LO-TO splitting of a single oscillator. The weak absorption at 800 cm^{-1} is associated with the SiOSi symmetric stretching, and the band at about 970 cm^{-1} has been assigned to the Si−O stretching of silanol groups.[2,24]

Acidified TEOS/H_2O Systems. CIR−IR difference spectra of the system TEOS/H_2O (1:80) at pH 2 (mixture minus aqueous HNO_3 of pH 2) as a function of reaction time, are shown in Figure 5. After 5.7 min of reaction, all bands except for the small one at 878 cm^{-1} in the spectra belong to TEOS, and as mentioned above, this small band is characteristic of EtOH. With increasing reaction time, more bands of EtOH become visible (1045 and 1085 cm^{-1}) and the intensity of the bands associated

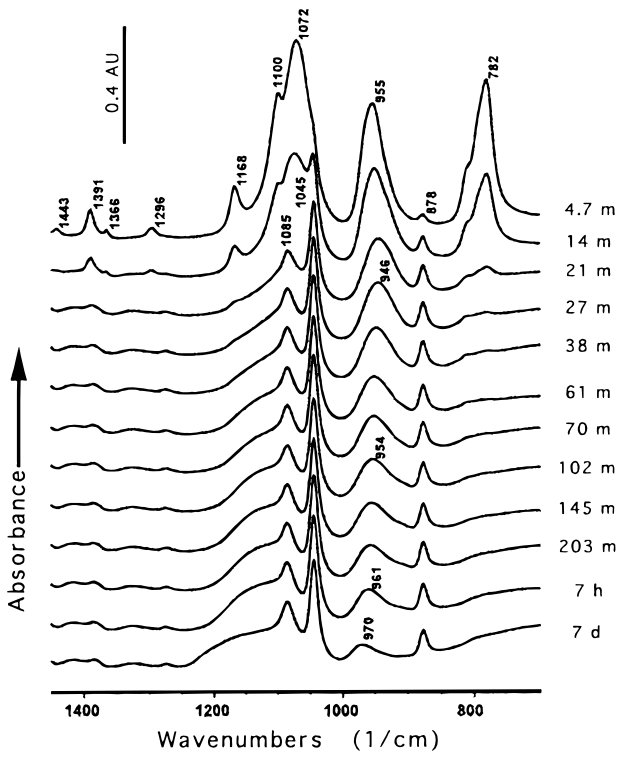

Figure 5. Difference spectra of pH 2 TEOS:H_2O (1:80) mixture (reaction mixture minus pH 2 aqueous HNO_3) at different times after mixing: m = minutes, h = hours, and d = days.

with TEOS at 1391, 1296, 1168, and 782 cm^{-1} decreases. Changes in the intensity of TEOS absorption at 1072 and 1100 cm^{-1} are difficult to follow due to their overlap with absorption bands of EtOH. The TEOS band at 955 cm^{-1} evolves to one with larger half-width and lower frequency (943 cm^{-1} in the spectrum at 21 min). With increasing reaction time, the intensity of this band decreases and moves again to higher frequency values (970 cm^{-1} after 7 days of reaction). At the same time there is an increase in the intensity of absorption between 1200 and 1100 cm^{-1}. Both the band at 943 cm^{-1} and the absorption band between 1200 and 1100 cm^{-1} can be associated with silicon oxide species produced in the hydrolysis of TEOS. According to the data presented in the preceding section, bands in the region of 1200−1100 and 970 cm^{-1} should be linked to the presence of SiO_2 while the band at 943 cm^{-1} is associated with monomeric silicic acid. Notice that the 943 cm^{-1} band is the only visible absorption that does not belong to the organic species, TEOS and EtOH, in the spectra at 21 and 27 min. Therefore, the silicon containing species at this time in the reaction are mainly in the form of $Si(OH)_4$. Between 38 min and 7 h of reaction time, the absorption maximum in this region shifts from 946 to 961 cm^{-1} and becomes increasingly less intense, wider, and more asymmetric, suggesting that the band observed in these spectra may have two components: absorption due to silicic acid (943 cm^{-1}) and absorption by silanols (970 cm^{-1}) present in tridimensional SiO_2. In summary, the spectra of Figure 5 seem to indicate that TEOS first hydrolyzes producing EtOH and $Si(OH)_4$, and that after 21 min there is very little TEOS left. The fact that none of these spectra show an absorption band between 1000 and 1050 cm^{-1}, characteristic of chain and sheet silicates,[26,29] seems to

(28) Baes, Ch. F.; Mesmer R. E. *The Hydrolysis of Cations*; John Wiley & Sons: New York, 1976; 342.

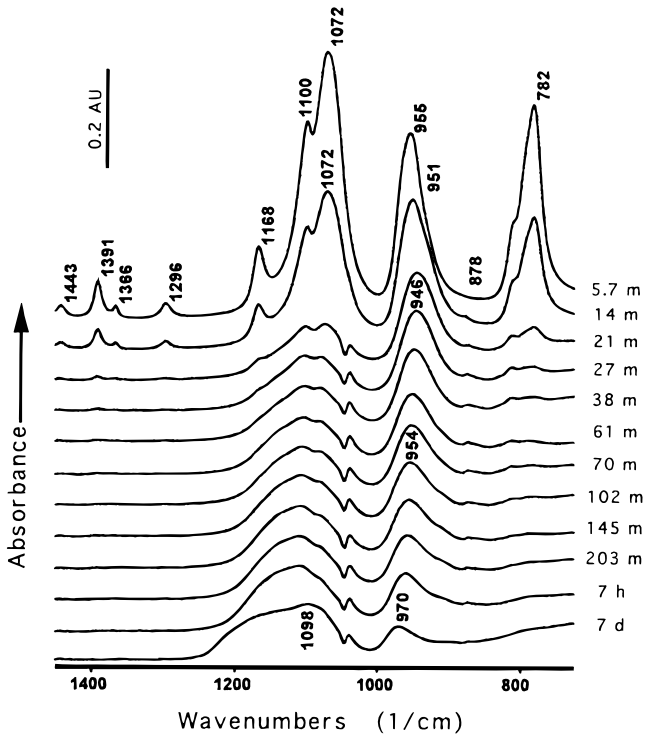

Figure 6. Subtraction result: Figure 5 spectra minus EtOH spectrum.

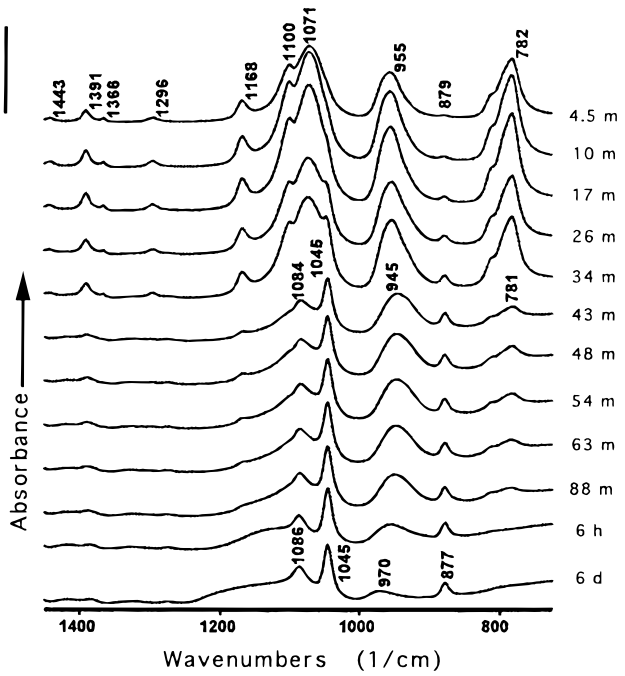

Figure 7. Difference spectra of pH 2.5 TEOS:H_2O (1:80) mixture (reaction mixture minus pH 2.5 aqueous HNO_3) at different times after mixing: m = minutes, h = hours, and d = days.

indicate that the $Si(OH)_4$ in solution precipitates as SiO_2, and that this process continues for over 7 h.

Figure 6 shows that the removal of the EtOH bands from the spectra of Figure 5 allows for better observation of the bands of condensed silica in the region of 1200−1050 cm^{-1}. However, the still strong absorption of TEOS at 1100 and 1072 cm^{-1} does not enable us to determine whether SiO_2 is present in the spectra at 5.7 and 14 min of reaction. Although bands of TEOS still appear in the spectrum after 21 min, the presence of tridimensional silica is already clearly manifested by the absorption increase in the region 1100−1150 cm^{-1}. Some spectra of Figure 6 show a small first-derivative-shaped perturbation, centered about the maximum of the most intense band of the EtOH (1045 cm^{-1}). The inability of performing a good spectral subtraction for this EtOH peak is related to the difference in concentration of EtOH in the reference (1 M) and in the sample (matrix effect). Fortunately, the presence of this perturbation does not affect the quality of the information in the spectra of Figure 6.

The removal of the TEOS bands from the spectra of Figure 6, by subtracting a spectrum of TEOS dissolved in EtOH, does not shed any new light on the presence of silica before 21 min of reaction since this operation results in first derivative profiles across the 1200 to 1050 cm^{-1} region. The reason dwells in a lack of matching in the shape and/or position of the absorption bands of TEOS dissolved in EtOH as compared to the ones of TEOS as micelles in aqueous medium (the hydrolysis reaction). Once again, the poor spectral subtraction is probably associated with the different degree of association of the TEOS molecules in each matrix. Peak fitting analysis, although time-consuming, in some instances is a safer method to identify individual components from a region of overlapping bands.[30] This method may answer the question on whether there is some silica absorption in the spectra obtained at 5.7 and 13.7 min of reaction time.

Figures 7 and 8 show spectra at different times of reaction for TEOS/H_2O systems hydrolyzed at pH 2.5 and 3, respectively. A visual inspection of the series of spectra in each of the Figures 5, 7, and 8 shows that the reaction products are the same for all three pH systems. However, the velocity of evolution is very different: the pH 2.5 system, after 88 min of reaction, has a spectrum similar to the pH 2 system after only 21 min of reaction. In contrast, the spectrum of the system at pH 3 at 73 min resembles the one of system at pH 2.5 at 17 min. There are some peculiarities in the system hydrolyzed at pH 3. While there is very little change in the spectra between 4 min of reaction time and 73 min, the spectra of the system change drastically between this time and 108 min. In these 35 min, the system of pH 3 evolves as much as the system of pH 2.5 between 16 min and 88 min. An explanation for these unexpected results will be found in the quantitative analysis of these spectra.

The Acidified TEOS/Methanol System. To compare the information that ATR−IR spectroscopy provides with those extracted from ^{29}Si NMR, we measured the IR spectra at different reaction times for a mixture of TEOS, methanol (MeOH) and water in a molar ratio 1:37:3, acidified with HNO_3 (10^{-2} F). In this study, the TEOS/H_2O molar ratio is lower than required for total hydrolysis (1:4).

The spectrum S1 of Figure 9 shows that, after 3 min of reaction, the absorption bands of TEOS (1168, 1103,

(29) Farmer, C. V. The Layer Silicates. In *The Infrared Spectra of Minerals*; Farmer, C. V., Ed.: Mineralogical Society: London, 1974.

(30) Dumas, R. L.; Tejedor-Tejedor, M. I.; Anderson, M. A. *J. Porous Mater.*, in press.

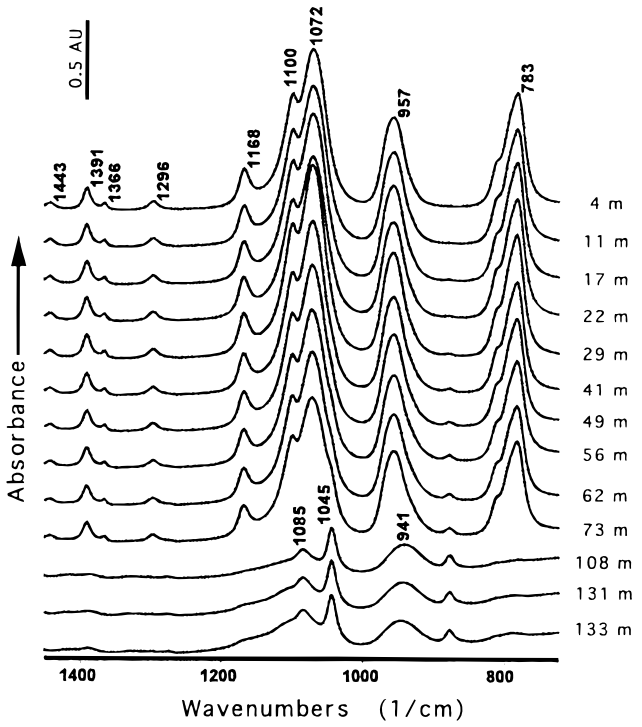

Figure 8. Difference spectra of pH 3 TEOS:H_2O (1:80) mixture (reaction mixture minus pH 3 aqueous HNO_3) at different times after mixing: m = minutes, h = hours, and d = days.

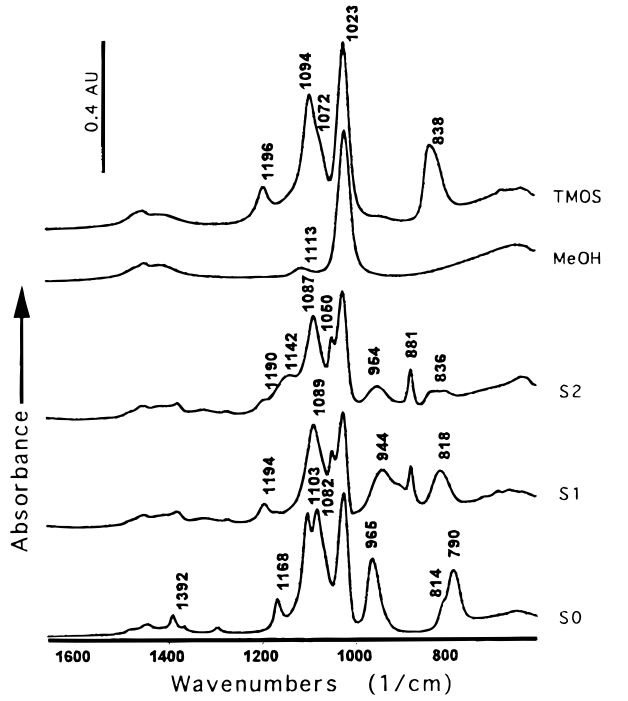

Figure 9. CIR−FTIR spectra of the hydrolysis of TEOS in MeOH: (SO) TEOS in methanol; TEOS in methanol + HNO_3 solution; (S1) 3 min after acidification; (S2) = (S1) 1 day later; (MeOH) neat methanol; (TMOS) TMOS in methanol. A spectrum of neat methanol multiplied by 0.8 was subtracted from all the spectra in this figure.

1082, 965, and 790 cm^{-1} in the spectrum of TEOS dissolved in methanol, Figure 9-S0) are not present. Moreover, there are new bands at 1194, 1089, 1050, 944, 881, and 818 cm^{-1} that are not related to any of the reactants (TEOS, MeOH, or H_2O). The peaks at 881 and 1050 cm^{-1} can be assigned to EtOH vibrations. The presence of EtOH in the spectrum of a 3 min old sample, S1, coincides with the absence of the absorption bands of TEOS. In addition, a comparative examination of this spectrum with the one of tetramethoxysilane (TMOS) in MeOH (Figure 9-TMOS), suggests the presence of this compound in the reaction mixture: 1194, 1089, and 818 cm^{-1} in the spectrum of S1 could be assigned to TMOS. This is not surprising since the exchange of an alkoxy group between the solvent and the alkoxysilane in this type of reactions has been reported by several authors.[3] However, the band at 944 and the shoulder at 914 cm^{-1} cannot be accounted for only by transformation of TEOS in TMOS. Also, the band at 818 cm^{-1} requires some explanation since its relative intensity, frequency at maximum, and profile do not totally match the ones of the TMOS band at 838 cm^{-1} in the Figure 9-TMOS spectrum. Alternatively, one could hypothesize that the set of bands attributed to TMOS, plus the bands near 946 cm^{-1} result from the absorption of a mixture of monomeric silane species, having a different number of EtO−, MeO−, and −OH groups. Bernards et al.[3] were able to identify by ^{29}Si NMR studies several monomeric species, with different number of $CH_3-CH_2-CH_2-O$-, CH_3-O-, and −OH bonded to the Si atom, in the early stages of the acid hydrolysis a mixture of TMOS:1-PrOH:H_2O (1:5:2).

In time, the TEOS/MEOH/H_2O mixture evolves. As shown in spectrum Figure 9-S2, by the intensity of the band at 881 cm^{-1}, the EtOH concentration reaches 1.76 M; this concentration is higher than the one in the mixture after 3 min of reaction (1.27 M). Spectrum S2 also shows that the absorption associated in the above discussion with monomeric silane species (bands at 1195, 944, and 818 cm^{-1}) decreases significantly while the absorption in the spectral region of condensed tridimensional silica increases (shoulder at 1142 cm^{-1}). In addition, the concentration of water, as measured from the water bending mode at 1636 cm^{-1}, decreases from 1.57 M initially to 0.65 M at 3 min of reaction and remains practically unchanged for the next 24 h.

Although an average molar composition of Si-containing species can be determined from these IR spectra (e.g.: in a 3 min old reacting mixture we calculated Si-$(-OH)_{1.64}(EtO-)_{1.73}(MO-)_{0.62}$), unlike ^{29}Si NMR spectroscopy, these studies do not allow for a more detailed speciation. Until there is a better IR spectra database for alkoxysilanes with different combinations of alkoxy and OH groups, we will not be in a position to perform better speciation studies. Other reasons for concern are: the potential lack of resolution due to the half-width of the IR bands next to a large number of bands produced by each species and the overlapping of the bands due to the reaction products with the very intense and sharp ones expected from the cosolvent.

3.3. Quantitative Interpretation of CIR−FTIR Spectra of Acidified TEOS/H_2O Systems. In the preceding section, we found that the spectra of these systems contain four chemical species, TEOS, EtOH, Si-$(OH)_4$, and amorphous silica particles; also, the concentration of each of these chemical species is a function of reaction time. The capability of correlating, in a quantitative manner, the concentration of the different spectral components with the intensity of their absorp-

tion bands should undeniably provide new insights into the reaction path of these systems.

Basic Principles of Quantitative ATR Spectroscopy: ATR can be used as a quantitative tool to measure species in solution/suspension in the same way that transmission spectroscopy is typically used. The reflectivity, R ($=I/I_o$), in ATR spectra can be expressed in terms of sample properties and concentration using a form of the Beer−Lambert law for absorbance in transmission, modified to accommodate reflectivity considerations:

$$-\log R = A = N\epsilon c d_e \tag{3}$$

here, A is the intensity of the ATR spectra, ϵ is the molar (decadic) absorption coefficient (SI units: $m^2\ mol^{-1}$), c is the molar concentration of the species in question (mol/m^3), N is the number of reflections made by the IR beam inside of the IRE, and d_e is the effective thickness. The term Nd_e is equivalent to the path length in transmission. The expression for pATR that obeys Harrick's thick film model to be used with the CIRCLE ATR accessory is given by eq 4,[31] where λ_1 is

$$A = \frac{N\epsilon c\lambda_1 n_{21} \cos\theta[(3 + n_{21}^2)\sin^2\theta - 2n_{21}^2]}{2\pi(1 - n_{21}^2)[(1 + n_{21}^2)\sin^2\theta - n_{21}^2](\sin^2\theta - n_{21}^2)^{1/2}} \tag{4}$$

the wavelength of the radiation in the IRE, θ is the angle of incidence, and n_{21} represents the ratio of the refractive index of the sample to that of the IRE.

Theoretically, as in the case of transmission spectroscopy, the plot of absorbance (A) vs concentration (c) should give a straight line, over a certain concentration range, for a given set of sampling parameters (N, n_1, and θ) as far as the refractive index of the sample, n_2, does not change with concentration. Therefore, quantitative information on a system can be gathered from the IR−ATR spectrum by the use of standards for calibrating the system. The use of working curves is an empirical method widely used in quantitative spectroscopy.

However, the use of calibration curves in ATR spectroscopy is valid only when the sample has the same refractive index as the standards. This condition is easily met for a wide range of concentrations of species in solution. In the case of stable suspensions of nanoparticles, the refractive index of the suspension is given by $[(V_{particles}/V_{suspension}) \times n_{particles}] + [(V_{solvent}/V_{suspension}) \times n_{solvent}]$. Hence, larger changes in the refractive index of a suspension as a function of solids concentration occur in systems for which $n_{particles}$ is very different from $n_{solvent}$. As an example, Table 2 shows how changes in the refractive index of a medium influence the intensity of absorption, A, by an analyte, for a given θ, N, vibrational mode ($\epsilon\lambda_1$), and concentration. This table also shows that particle concentration in aqueous suspensions of SiO_2 and TiO_2 (the refractive indices are close to 1.5 for SiO_2 and to 2.54 for TiO_2(anatase)) influences the refractive index of the suspension. In the case of larger colloidal particles in suspension, the situation can be more complex, and discussion of these systems is beyond of the scope of this paper.[31]

Table 2. Influence of the Solids Concentration on the Refractive Index of a Suspension and Thus on the Intensity of Absorption of the Species in the Media

nanoparticle nature	concentration in water: *c*, g/L	concentration in water: *c*, vol %	suspension refractive index[a] (n_s)	$A(n_s)/A(n_w)$[b]
SiO_2 ($d = 2.5$ g/cm^3;	50	2	1.332	1.00
$n = 1.50$)	100	4	1.337	1.01
	200	8	1.343	1.02
TiO_2 (anatase)	50	0.5	1.336	1.02
($d = 3.8$ g/cm^3;	100	2.6	1.361	1.07
$n = 2.54$)	200	5.2	1.393	1.15

[a] Refractive index of water in nonabsorbing region (n_w) = 1.33. [b] $A(n_i)$ = intensity of absorption for a system when the refractive index is n_i.

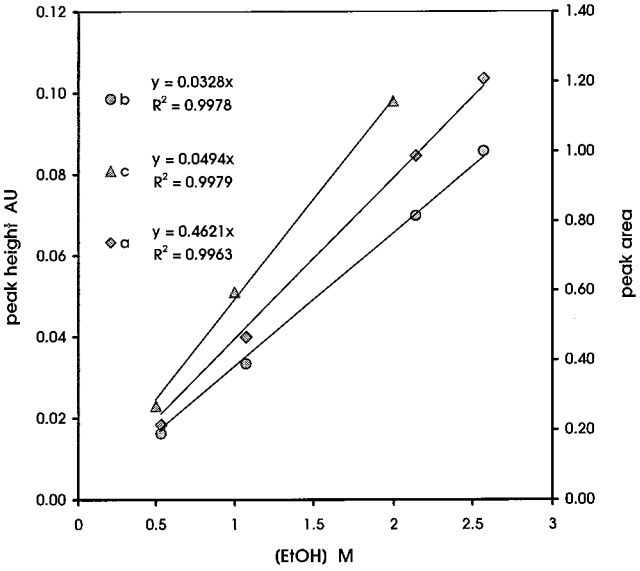

Figure 10. Calibration curves for EtOH in both water and methanol using the peak at 878/881 cm^{-1}: (a) in water, peak area; (b) in water, peak height; (c) in methanol, peak height.

Deviation from Beer's law in transmission FTIR is mainly caused by insufficient resolution, and by nonideal behavior of the sample itself. For bands of weak and medium intensity (<0.7 au), band intensity can be linearly proportional to sample concentration even for low resolution. The nonideal behavior of a sample is, in general, linked to changes in the degree of intermolecular association as a function of its concentration. In ATR−FTIR spectroscopy, nonlinearity in absorption vs concentration working curves may also occur due to changes in the refractive index of the sample with varying concentration.[32]

CIR−IR Working Curves for the Different Components of Acidified TEOS/H_2O Samples. Parts a and b of Figure 10 show the calibration curves of EtOH in H_2O for concentrations between 0.5 and 2.5 M, the concentration range expected for the EtOH in the acidified TEOS/H_2O systems studied in this paper. Parts a and b of Figure 10 are the result of plotting the integrated intensity/intensity at maximum of the peak at 878 cm^{-1}

(31) Tickanen, L. D.; Tejedor-Tejedor, M. I. *Langmuir* **1997**, *13*, 4829.

(32) Muller, G. J.; Abraham-Fuchs, K. Matrix Dependence in Single and Multilayer Internal Reflection Spectra. *In Internal Reflection Spectroscopy*; Mirabella, F. M., Jr., Ed.; Marcel Dekker: New York, 1993.

Table 3. CIR−FTIR Calibration Curve for Ethanol in Water

[EtOH] (mol/L)	peak height at 878 cm^{-1}	av peak height	σ_H	area of the peak at 878 cm^{-1}	av peak area	σ_A
0.533	0.0160	0.0163	0.0004	0.2080	0.2153	0.011
	0.0160			0.2050		
	0.0160			0.2110		
	0.0170			0.2320		
	0.0163			0.2206		
1.071	0.0330	0.0334	0.0006	0.4610	0.4672	0.012
	0.0330			0.4560		
	0.0330			0.4640		
	0.0342			0.4860		
	0.0340			0.4689		
2.141	0.0700	0.0698	0.0004	0.9910	0.9860	0.015
	0.0700			1.0050		
	0.0690			0.9650		
	0.0700			0.9910		
	0.0699			0.9780		
2.569	0.086	0.0856	0.0005	1.217	1.2062	0.011
	0.086			1.217		
	0.086			1.205		
	0.085			1.197		
	0.085			1.195		

vs the concentration of EtOH. To study the precision of the technique, a set of four standards was measured five times on several different days. Between runs, the sample holder was removed from the CIRCLE cell and reinstalled. Therefore, the standard spectra obtained on different days employed different background and references in their data reduction. The same physical standards were used in three of the runs. In the other two, we used newly prepared standard solutions.

Table 3 displays the concentration of the standards, the absorption intensity at 878 cm^{-1}, the integrated intensity of this peak, and the standard deviation for each standard solution data set. The least-squares method was used to fit a straight line through the experimental points in parts a (area) and b (height) of Figure 10. Since the spectrum of water (blank) was subtracted from the one of EtOH in water, we have fit an equation of the form $y = bx$. The proportion of total variation as given by the square of the multiple correlation coefficient, R^2 (0.9963 and 0.9978) is excellent. Furthermore, Table 3 shows that the standard deviation is constant over this range of concentration. However, the pure error test shows better linearity for peak areas.

The calibration curve of EtOH in methanol, Figure 10c, has a different "operative" molar absorption coefficient (0.0494) than the curve for EtOH in H_2O (0.0328). Since the same experimental setting was used to obtain the spectra of EtOH in both media, the difference in the "operative" molar absorption coefficients should correspond to a difference in the true molar absorption coefficient. This matrix effect is probably caused by the different degrees of association of the EtOH molecules with each of the solvents. Since this effect can be large, the standards used in the calibration curve should be prepared in the same solvent as that of the sample. Therefore, for the quantitative analysis of the EtOH released during the hydrolysis of alkoxides in rich water media, one should use the absorption coefficient of EtOH in water.

Parts a and b of Figure 11 correspond to the calibration curves of TEOS in EtOH. These were plotted using the absorption at maximum of two different bands of

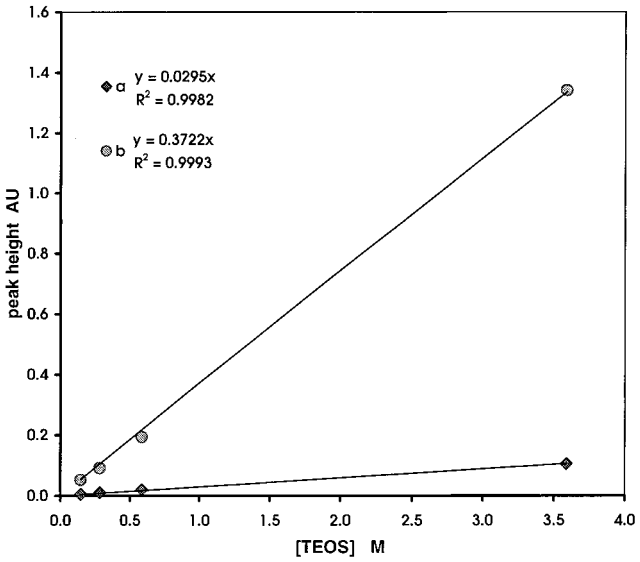

Figure 11. Calibration curve for TEOS in EtOH: (a) using the height of the peak at 1296 cm^{-1}; (b) using the height of the peak at 785 cm^{-1}.

the TEOS spectra, 1296 and 785 cm^{-1}. We can fit a straight line of the type $y = bx$ through both data sets with values for R^2 of 0.9992 and 0.9993, respectively. Thus, for the range of concentrations 0.1−0.6 M, the use of either of these two bands provides good reproducibility and linearity. As expected, the band with the highest relative intensity, 785 cm^{-1}, shows the higher sensitivity and reproducibility. However, band overlapping and also the concentration level of TEOS will ultimately determine the choice of analytical band.

Moreover, we have measured the absorption intensity due to the SiOSi asymmetric stretching vs the concentration of amorphous silica in aqueous suspension. We performed this analysis for two different types of amorphous silica, originating from the acidic (AH) and basic hydrolysis (BH) of TEOS. Plots of intensity of absorption at 1119 and 1102 cm^{-1} for BH and AH silica, respectively, vs concentration of silica in suspension are given in parts a and b of Figure 12. The slope of the least-squares fitted straight line for the silica from the basic hydrolysis is 0.337, while that for the silica obtained from acidic hydrolysis is 0.179. Partc c and d of Figure 12 show the relationship between SiO_2 concentration and the integrated intensity in the region 1261−912 cm^{-1} for both BH and AH silica. The statistical analysis of these data shows that the precision of this method for measuring the concentration of silica in suspension is comparable to that of the species in solution that we described above and, in all cases, is excellent. Figure 12 shows that structural differences in amorphous silica (differences in the angle between the Si tetrahedrons) influence mainly the molar absorption coefficient of the Si−OSi stretching at the wavenumber of maximum absorption and also, although to a much lesser extent, the integrated adsorption coefficient in the region 1261−912 cm^{-1} (includes Si−OSi and Si−O− modes). Therefore, the SiO_2 of the suspensions used as standards should have structural properties similar to that of the sample; the use of integrated intensity is more safe than the use of intensity of absorption at a given wavenumber in the quantitative analysis of SiO_2.

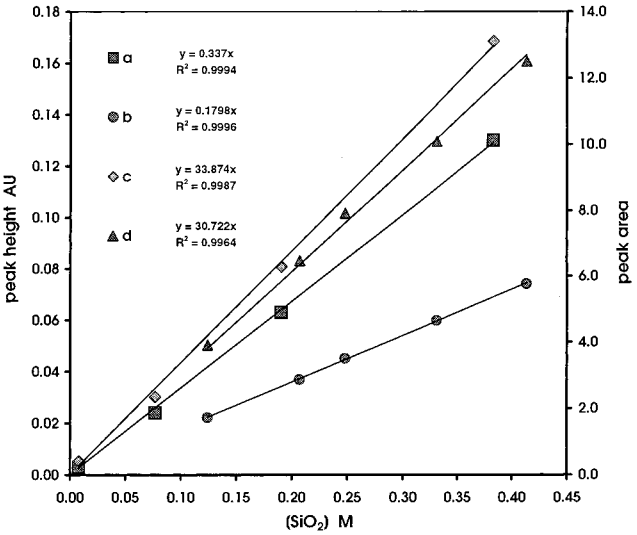

Figure 12. Calibration curve for amorphous SiO_2 particles in aqueous suspension, originating from the acidic hydrolysis (AH) and basic hydrolysis (BH) of TEOS: (a) BH, using the height of the peak at 1119 cm^{-1}; (b) AH, using the height of the peak at 1102 cm^{-1}; (c) BH, using the integrated intensity of the peaks in the region 1261−912 cm^{-1}; (d) AH, using the integrated intensity of the peaks in the region 1261−912 cm^{-1}.

It is not trivial to construct an IR calibration curve for dissolved silicic acid at room temperature. The concentration of $Si(OH)_4$ should be lower than 2×10^{-3} M (solubility of amorphous silica) to avoid the presence of other species and therefore to be able to identify total concentration of Si in solution (as measured by other analytical techniques such as ICP vs primary standards) with the concentration of $Si(OH)_4$. Therefore, to measure the concentration $Si(OH)_4$ in systems in which the solubility limit is exceeded (metastable solutions) one has to extrapolate "operative" molar absorption coefficients obtained for lower concentration ranges. For a $Si(OH)_4$ concentration of 2×10^{-3} M, the S/N ratio, using the intensity at the maximum of the 943 cm^{-1} band, is approximately 15. If one dilutes this concentration by 50%, the band intensity will dangerously approach the detection limit. For this reason, we obtained the "operative" molar absorption coefficient by measuring the absorption intensity from four different spectra of a solution 1.35 mM (as measured by ICP) in $Si(OH)_4$. The absorption intensity of this silica solution at 942 cm^{-1} is 0.00059 ± 0.00002 au.

Concentration of Chemical Species Present in the Acidified TEOS/H_2O Systems. The integrated intensity of the EtOH band at 878 cm^{-1} in the spectrum of TEOS/H_2O at pH 2, taken after 38 min of reaction, Figure 5, yields a concentration of EtOH of 2.08 ± 0.03 M. This value was calculated using the relation: area of the band = 0.462 × [EtOH], obtained from Figure 10a. This concentration of EtOH is the same as that in a 5 day old mixture and corresponds to a TEOS concentration of 0.520 ± 0.008 M. This is very close to the initial concentration of TEOS in this system, 0.56 F.

Measurements of the intensity of absorption at 946 cm^{-1} in the spectra of Figure 6 show that the concentration of $Si(OH)_4$ in the mixture reaches a maximum value of 0.39 M after 21 min of reaction, accounting for 70% of the Si in the system (0.56 F). We do not know the accuracy of this measurement since it must be calculated using standards in a range of concentration below 2 mM. There is not an easy way to correct this problem, since solutions with higher concentrations of $Si(OH)_4$ are metastable and consequently contain a mixture of different silica species. A concentration value lower than 0.56 M makes sense since the spectrum of this sample, in Figure 6, shows that a certain amount of TEOS remains unreacted and SiO_2 is already present.

The spectrum taken after 38 min of reaction, Figure 6, shows that the concentration $Si(OH)_4$ is already lower than after 21 min of reaction while the concentration of SiO_2 has increased. After 7 days of reaction, the concentration of SiO_2, calculated from the integrated intensity of absorption in the region 1261−912 cm^{-1}, is 0.53 M. This value for the Si concentration is not significatively different from that calculated from the EtOH concentration (0.52 M) given the precision of analysis for both EtOH and SiO_2. Therefore, we can say that, after 7 days, the reaction products of the TEOS hydrolysis are SiO_2 and ethanol. Although some $Si(OH)_4$ should be present, this is not obvious in the IR spectrum (946 cm^{-1}) of a 7 day old sample. The band of $Si(OH)_4$ probably appears in the spectrum as a very small contribution to the low-frequency wing of the band of silanols at 970 cm^{-1} (ICP measurements of dissolved silica at equilibrium with these SiO_2 sols yield concentration values near 1.7 mM).

We did not attempt to quantify the changes in the concentration of TEOS as a function of reaction time since this alkoxide does not mix with water but forms unstable emulsions. It will be nearly impossible to obtain an "operational molar absorption coefficient " from a calibration curve that can ensure any accuracy of analysis.

The mass balance for the molar ratio of the reaction products, [EtOH]/[SiO_2], is very good (stoichiometry = 4; stoichiometry from these analyses = 3.96). The initial concentration of TEOS, calculated from the reaction products, is 0.52_5 M, while the initial formal concentration is 0.56 M. This small discrepancy may be caused by a difference between the formal and the real value of the concentration of TEOS. However, since we found formal concentrations to be very close to that obtained from the analysis of C (by TOC) and Si (by ICP) for new stock bottles, the matrix shift effect[32] is a more likely explanation for the numerical discrepancy.

3.4. Kinetics of Hydrolysis. The kinetics of TEOS hydrolysis can be expressed as the variation in concentration of EtOH in the reaction mixture as a function of time. The results of these studies are shown in Figure 13 for the hydrolysis of TEOS at pH 2, 2.5, and 3. In the system at pH 2, the concentration of EtOH changes linearly with time and reaches, after approximately 21 min, a plateau at 2.10 M. This value corresponds to the total hydrolysis of TEOS, and the shape of the curve suggests a first-order reaction. Although, in both cases, the concentration of EtOH reaches the same maximum value, the production of EtOH in the mixture at pH 3 is slower than at pH 2. Furthermore, the shape of the curve at pH 3 is very unusual and cannot be fit by either zero-, first-, or second-order kinetic models.

The explanation for this unusual shape can be found in a comparative study of the intensity of the absorption

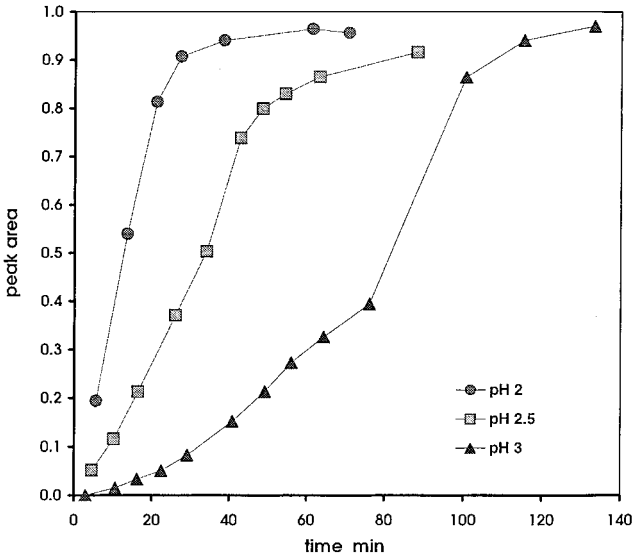

Figure 13. Kinetics of hydrolysis for acidified TEOS:H_2O (1:80) systems at different values of pH. Inferred from the area of the peak of EtOH at 878 cm^{-1}.

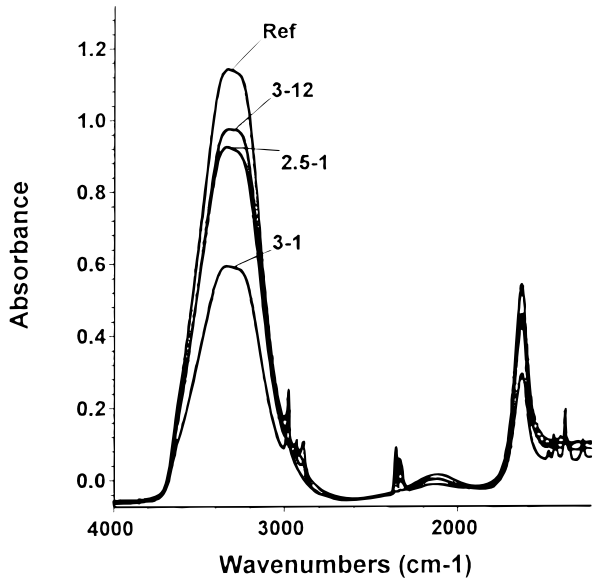

Figure 14. CIR−FTIR spectra: (3−1) TEOS:H_2O (1:80) mixture, pH 3, reaction time = 4 min; (2.5−1) TEOS:H_2O (1:80) mixture, pH 2.5, reaction time = 4.5 min; (3−12) TEOS:H_2O (1:80) mixture, pH 3, reaction time = 133 min; (Ref) water.

bands of water (major constituent) in the spectra of the reaction mixtures at different stages of reaction, and in the spectrum of pure water, Figure 14. The intensity of the water bands is expected to be larger in the spectrum of pure water than in the spectra of the TEOS/water systems at any of the three pH values mentioned above since the water molarity in the latter systems is approximately 86% of that in pure water. However, the spectra in Figure 14 show that there is large variability in the intensity of the water bands in the spectra of the TEOS/water samples: The intensity of water bands in the spectrum "3−12" is close to 86% of the intensity in the spectrum of pure water. This spectrum is representative of the TEOS/water samples at all three values of pH that have been reacting for at least 100 min. The intensity of absorption in spectrum "2.5−1" is only 78% of that of pure water. This spectrum is representative of the TEOS/water system at pH 2 before 20 min of

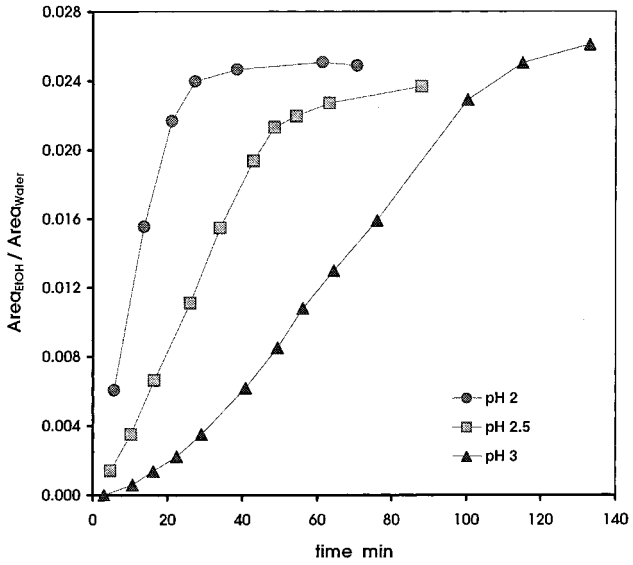

Figure 15. Kinetics of hydrolysis for acidified TEOS:H_2O (1:80) systems at different values of pH. Inferred from the following ratio: area of EtOH at 878 cm^{-1} area of H_2O at 1636 cm^{-1}.

reaction and also represents the system at pH 2.5 before 40 min of reaction. The spectrum "3−1" stands for the system at pH 3 before 100 minutes of reaction, and its intensity is only 55% that of pure water.

The above values and variability of the intensity of absorption of the water bands as a function of reaction time cannot be attributed to changes in the molarity of water due to reaction. The stoichiometry of the completed hydrolysis /condensation of TEOS reaction, at any of the three pH values, predicts the consumption of 2 mol of water per mole of TEOS converted into SiO_2. Therefore, in these systems (concentration of TEOS = 0.56 M) the water molarity should decrease approximately 2% upon reaction completion. However, Figure 15 shows just the reverse. Furthermore, although the water molarity in the initial stages of the reaction should not depend on the pH of hydrolysis, Figure 15 shows that the intensity of the water bands for a 3 min old sample at pH 3 ("3−1") is only 70% that of the intensity in the spectra of a sample 4 min old taken at pH 2.5 ("2.5−1").

We believe that these anomalous changes in intensity of the water bands are associated with the physical nature of the TEOS/water mixture, in conjunction with the optical principles behind ATR spectroscopy. Not only does the intensity of an absorption band in ATR spectroscopy depend on the parameters given in eq 4, but also this equation is only valid when the sample is homogeneously distributed as a thick layer (much thicker than the sampling depth) around the IRE (ZnSe cylindrical crystal in this study). Due to the low solubility of TEOS in water, during the first stages of hydrolysis, the two components form an emulsion in which the size of the TEOS micelles depends on the stirring strength. A stable suspension of micelles covering the IRE can be regarded for the purpose of IR−ATR spectroscopy as an homogeneous thick film and the intensity of the bands should be related to the concentration of species through eq 4. However, if the micelles of TEOS in the suspension, even when being stirred, have some preference for the IRE surface, they can form

a layer of pure TEOS between the IRE and the micellar suspension. This sample geometry will yield spectra with enhanced intensities of absorption for the bands of TEOS and depleted intensities of absorption for the water and species in the aqueous phase. This is actually what is observed in the spectra of Figure 15. In the system at pH 3, the water and EtOH bands are less intense than expected while micelles of TEOS are present in the suspension, and the bands relax to normal values after the hydrolysis is finished. This model also explains the unusual shape of the kinetic curve of EtOH formation in the system at pH 3. The question remains regarding the role of pH in determining the magnitude of TEOS partitioning between the IRE and the aqueous phase. To answer this question, we measured the electrophoretic mobility of micelles in the system at the three different pH values used for hydrolysis. We found that at pH 2, the micelles are positively charged with a mobility of 1.8×10^{-8} m^2 V^{-1} s^{-1} after 2 min of reaction, changing to 1.6×10^{-8} after 4 min. In the system at pH 3, the micelles are already negatively charged and show smaller mobilities (between -0.7×10^{-8} and -0.1×10^{-8}). Since we know that the pH_{iep} for the ZnSe is around 3, these results could explain why the tendency for the TEOS micelles to coalesce and deposit on the IRE is much smaller in the system at pH 2 than at pH 3.

Now we can see that it is virtually impossible to quantify changes in the TEOS concentration along the reaction pathway. Under conditions in which a layer of TEOS covers the IRE, one cannot calculate the concentration of EtOH using the calibration curves of Figure 10, since the relationship between intensity of a band and concentration obeys different mathematical equations for each system. However, we should still be able to follow the kinetics of EtOH formation by plotting the relative intensity of the ethanol band with respect to one of the water bands against the reaction time. For this methodology to be valid, we have to assume that all the EtOH is in the aqueous phase. Indeed, the intensity of the spectra of all the species in the aqueous phase should be equally affected by the presence of a film of TEOS on the IRE surface. Therefore, the water in the sample can be used as an internal standard. Figure 15 shows the kinetics of EtOH formation using the intensity of 880 cm^{-1} band of EtOH relative to the 1636 cm^{-1} of water for the systems at pH 2 and pH 3; the shape of the curve at pH 2 is the same as the one obtained using the absolute intensity of this band of EtOH (Figure 13). However, the curve obtained for the system at pH 3 using the relative intensity is very different from that obtained using its absolute intensity (Figure 13). It is much smoother and, as in the case of the system at pH 2, is similar to the shape expected for first-order kinetics.

Although it seems that the experimental data easily fit a first-order kinetic model, there is no practical value of calculating its model constants since the reaction rate will depend on the size of the micelles and therefore on such nonintrinsic parameters as stirring speed.

4. Conclusions

This paper demonstrated the effectiveness of ATR−FTIR spectroscopy to provide "in situ" qualitative data regarding the species present during the hydrolysis and condensation of TEOS in aqueous media. These spectra undoubtedly showed that the concentration of TEOS decreases concurrently with the generation of EtOH and $Si(OH)_4$ and that later in the reaction, the concentration of $Si(OH)_4$ decreases at the same time that SiO_2 increases.

Calibrating the system with standards enabled us to perform the "in situ" quantitative analysis of components in solution, such as EtOH and $Si(OH)_4$, and also of those in suspension, such as amorphous SiO_2. Statistic analysis of the data used in the calibration curves of EtOH in water and in methanol, TEOS in ethanol, and SiO_2 in water showed good linearity and reproducibility in the range of concentrations used in these studies. The effect of the matrix on the intensity of absorption can be very large, as illustrated by the calibration curves of ethanol in water and in methanol.

In some of these systems (for example, TEOS hydrolysis at pH 3 during the first 100 minutes of reaction), the micelles coalesce on the IRE (ZnSe crystal). In these cases quantitative analysis cannot be carried out by using the above-mentioned methodology of working curves. In the spectrum of these mixtures, TEOS will be over represented, while the opposite will be true for the rest of the sample components. The use of the bending mode of water as an internal standard may in some cases allow the calculation of the concentration of species in the aqueous phase.

The spectra in this paper have been measured with a collection time of 2 min (200 scans). However, measurement times no larger than 30 s still produce very good signal-to-noise ratio. Thus, this technique is a very good candidate for studying the kinetics of reaction in these systems.

ATR−FTIR spectroscopy also can provide "in situ" information on the hydrolysis reaction path of TEOS dissolved in alcohol. However, at present, the speciation of newly formed silanes such as $Si(OEt)_x(OM')_y(OH)^{4-x-y}$ or small oligomers is not as dependable as identification using ^{29}Si NMR spectra.

CM980146L